PHILOSOPHICAL TRANSACTIONS OF THE ROYAL SOCIETY A

Phil. Trans. R. Soc. A (2008) **366**, 397–408
doi:10.1098/rsta.2007.2097
Published online 2 August 2007

Coupled and forced patterns in reaction–diffusion systems

By Irving R. Epstein*, Igal B. Berenstein, Milos Dolnik, Vladimir K. Vanag, Lingfa Yang and Anatol M. Zhabotinsky

Department of Chemistry and Volen Center for Complex Systems, Brandeis University, MS 015, Waltham, MA 02454, USA

Several reaction–diffusion systems that exhibit temporal periodicity when well mixed also display spatio-temporal pattern formation in a spatially distributed, unstirred configuration. These patterns can be travelling (e.g. spirals, concentric circles, plane waves) or stationary in space (Turing structures, standing waves). The behaviour of coupled and forced temporal oscillators has been well studied, but much less is known about the phenomenology of forced and coupled patterns. We present experimental results focusing primarily on coupled patterns in two chemical systems, the chlorine dioxide–iodine–malonic acid reaction and the Belousov–Zhabotinsky reaction. The observed behaviour can be simulated with simple chemically plausible models.

Keywords: reaction–diffusion; pattern formation; coupled systems

1. Introduction

Interest in the behaviour of coupled oscillators dates back at least as far as Huygens' seventeenth century observations of synchronization of clocks on a wall. More recent studies of the menstrual cycles of women living in close proximity and of the flashing of fireflies provide other fascinating examples of the synchronization of coupled temporal oscillators. When oscillators do not synchronize, they can produce other qualitatively different behaviours including: beating, the generation of the frequency difference when two oscillators with incommensurate frequencies are coupled; oscillator death, the cessation of oscillations on coupling two oscillators; rhythmogenesis, the initiation of oscillations by coupling two steady-state systems; and chaos, an aperiodic behaviour that emerges when two periodic subsystems are coupled. Much attention has also been devoted to coupled bistable systems, particularly to the issue of propagation failure, i.e. the question of how strong the coupling must be in a string of bistable elements in order for a switching in the state of one to cause all the others to flip. Studies of forced oscillators have explored, among other issues, the phase resetting produced by imposing an external stimulus at different times and with different amplitudes during the oscillatory cycle, and the possibility of pushing a chaotic oscillator into a periodic behaviour by imposing a weak external signal ('control of chaos').

* Author for correspondence (epstein@brandeis.edu).

One contribution of 15 to a Theme Issue 'Experimental chaos I'.

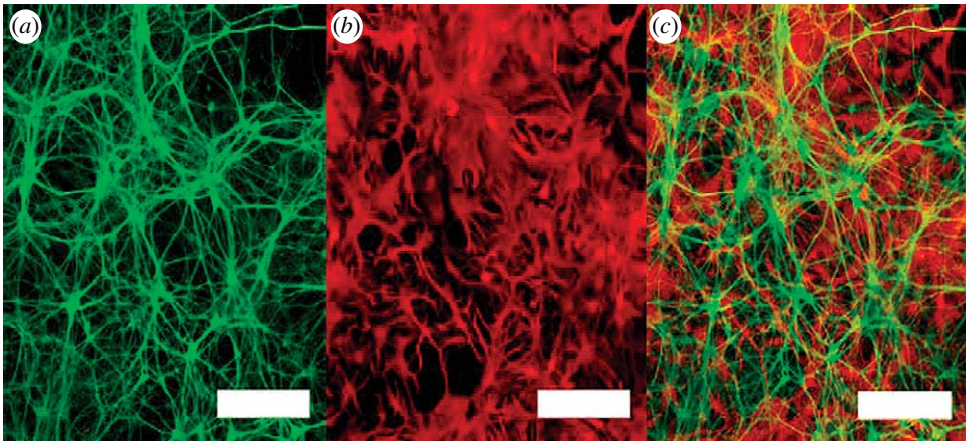

Figure 1. Network of interspersed neurons and glia in a dissociated rat hippocampus culture. (*a*) Imaging the neural network only. (*b*) Imaging the glial network only. (*c*) View showing the intertwining of the two networks. Scale bars, 200 μm. (Courtesy of Anna Lin, Duke University.)

2. Coupled patterns: experiments

While not as well studied as coupled temporal oscillators, systems in which spatial or spatio-temporal patterns are linked together are of considerable importance in a variety of contexts. These include: biological development, where two or more organs or organ systems may evolve simultaneously, sharing common resources; neural networks, either in computational or in actual brains, where patterns in one layer or column of neurons may interact with patterns in another; social and economic systems, in which patterns of activity in different subpopulations or sectors may affect one another; and ecology, where the spatial distribution of an organism can influence that of a competitor, predator or prey species. An example of two interacting patterns, one of glial cells and the other of neurons, in a slice from the hippocampal region of a rat brain is shown in figure 1.

We present here results on several reaction–diffusion systems that consist of relatively simple chemical reactions that generate patterns in spatially distributed media. We consider various means of achieving coupling between patterns in these systems.

(*a*) *The CDIMA system*

The first system of interest is the chlorine dioxide–iodine–malonic acid (CDIMA) reaction (Lengyel *et al.* 1990*a*). This reaction and the related chlorite–iodide–malonic acid (CIMA) reaction (De Kepper *et al.* 1982) were the first to generate experimental evidence of Turing structures (Castets *et al.* 1990), the spatially periodic, temporally stationary reaction–diffusion patterns proposed over half a century ago as a possible mechanism for biological differentiation (Turing 1952). In pattern formation studies, the reactants are typically distributed within a thin layer of gel (usually polyacrylamide or agarose) and a small quantity of an indicator, a substance that reversibly forms a coloured complex with the iodine-containing species, is added to enhance contrast. The Turing patterns arise because the complex is typically larger and much less

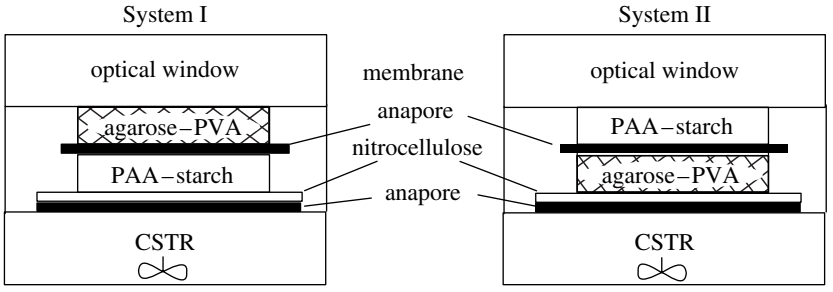

Figure 2. Experimental arrangement for studying coupled patterns in the CDIMA system. CSTR is a continuous flow stirred tank reactor containing the reactants. The system is viewed through the upper optical window. The lower gel layer is separated from the CSTR by two membranes. The two gel layers may be separated by a second anapore membrane (weak coupling case). Adapted from Berenstein *et al.* (2004). CDIMA, chlorine dioxide-iodine-malonic acid; CSTR, continuous stirred-tank reactor; PAA, polyacrylamide; PVA, polyvinyl alcohol.

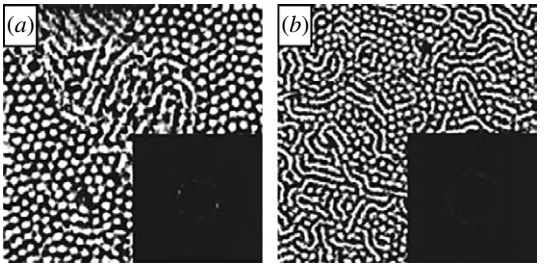

Figure 3. Turing patterns in single-layer experiments. (*a*) Agarose gel: $[I_2]_0 = 0.37$ mM, $[MA]_0 = 1.80$ mM, $[ClO_2]_0 = 0.136$ mM; PVA = 1 g l^{-1}. Subscript 0 indicates concentration in the CSTR. (*b*) PAA–starch (1 g l^{-1}) gel: $[I_2]_0 = 0.35$ mM, $[MA]_0 = 1.91$ mM, $[ClO_2]_0 = 0.156$ mM. Image sizes: 10×10 mm. Fourier spectra, shown as insets, give wavelengths of (*a*) 0.32 mm and (*b*) 0.25 mm. Adapted from Berenstein *et al.* (2004). CSTR, continuous stirred-tank reactor.

mobile in the gel than the other species (Lengyel & Epstein 1991), which effectively slows the diffusion of iodine, the activator in the CDIMA and CIMA reactions. Turing (1952) showed that pattern formation requires that the activator diffuse significantly less rapidly than the inhibitor, a condition difficult to fulfil in ordinary aqueous systems involving small molecules like those in the CDIMA system. Pattern formation in the CDIMA system is well described by a simple two-variable model, known as the Lengyel–Epstein model (Lengyel *et al.* 1990*b*), that takes into account both the nonlinear kinetics of the underlying system and the complex formation between the activator species and the gel-bound indicator.

Experiments on coupled patterns in the CDIMA system have used the configuration illustrated in figure 2, where two thin gel layers with different compositions are placed in contact, either directly or through a membrane (Berenstein *et al.* 2004). One gel is composed of agarose, with polyvinyl alcohol (PVA) as an indicator. The other consists of polyacrylamide (PAA), with starch as the indicator. The complex with PVA is red, while that formed with starch is blue, so that, by using filters of appropriate colours, one can view separately the patterns formed in the two layers. Experiments were conducted in two

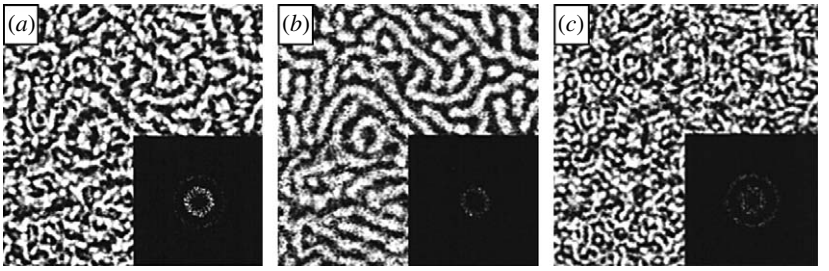

Figure 4. Superposition patterns with weak coupling in System I. (*a*) Unfiltered image (summation of both layers). Same pattern seen through filter transparent to (*b*) blue light (in agarose gel) and (*c*) red light (in PAA gel). Image sizes: 10×10 mm. Fourier spectra, shown as insets, give wavelengths of 0.54 and 0.23 mm. $[I_2]_0 = 0.37$ mM, $[MA]_0 = 1.80$ mM, $[ClO_2]_0 = 0.145$ mM; PVA = 1 g l^{-1}. Adapted from Berenstein *et al.* (2004).

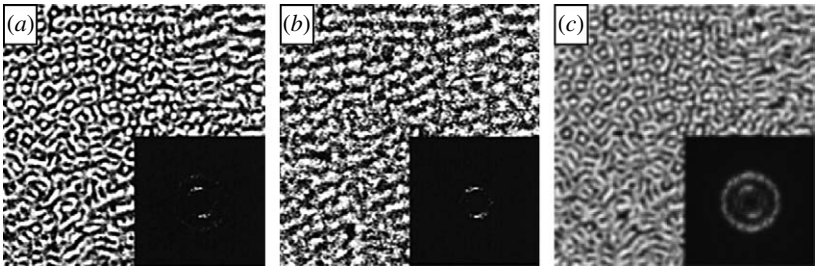

Figure 5. Superlattice patterns with strong coupling in System I. (*a*) Unfiltered image (summation of both layers). Same pattern seen through filter transparent to (*b*) blue light and (*c*) red light. Image sizes: 10×10 mm. Fourier spectra, shown as insets, give wavelengths of 0.46 and 0.25 mm. $[I_2]_0 = 0.37$ mM, $[MA]_0 = 1.80$ mM, $[ClO_2]_0 = 0.144$ mM; PVA = 1 g l^{-1}. Adapted from Berenstein *et al.* (2004).

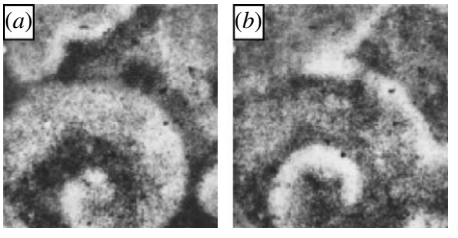

Figure 6. Travelling waves in System II. Agarose layer only is shown. Images obtained with blue filter. Image sizes: 10×10 mm. $[I_2]_0 = 0.35$ mM, $[MA]_0 = 1.90$ mM, $[ClO_2]_0 = 0.157$ mM; PVA = 1 g l^{-1}, [starch] = 1 g l^{-1}. Image in (*b*) is taken 50 s after (*a*). Adapted from Berenstein *et al.* (2004).

configurations: System I with the PAA layer closer to the continuous stirred-tank reactor and System II with the agarose layer closer. We were also able to consider two cases of coupling: strong coupling where the two gel layers were in direct contact and weak coupling where they were separated by an anapore membrane.

Typical results are shown in figures 3–6. In figure 3, we present the Turing patterns observed in single uncoupled layers of each of the gels. Figure 4 shows the patterns found in the weak coupling case with the configuration of System I. The pattern in the agarose layer (figure 4*b*) is essentially unaffected by the presence of the PAA layer, while the latter shows modulation by the former. The strong coupling case, shown in figure 5, demonstrates a new phenomenon. In figure 5*a*,*c*,

we find a superlattice 'white eye' pattern containing two distinct spatial wavelengths (see Fourier transforms), which arises from the nonlinear interaction between the patterns in the individual layers. The observed wavelengths have been modified by the coupling and are now closer to one another than in the weak coupling case.

Reversing the order of the layers, which affects the relative concentrations of reactants in the two layers, tends to favour travelling waves in the agarose layer, as shown in figure 6, over the stationary patterns that dominate in System I, though stationary patterns can be observed in System II at other concentrations.

(*b*) *The BZ–AOT system*

The Belousov–Zhabotinsky (BZ) reaction is the prototype system for studying pattern formation in reaction–diffusion systems. It consists of the oxidation and bromination in sulphuric acid of an organic substrate such as malonic acid (MA, $CH_2(COOH)_2$) in the presence of a redox-active catalyst like cerium ion or ferroin. In aqueous solution, it displays a rich variety of spatio-temporal behaviours, including periodic oscillation, chaos and travelling waves. Vanag and Epstein have developed a modification of the BZ system in which the reaction is carried out in a thin layer of a reverse microemulsion containing water, oil (usually octane) and a surfactant, sodium bis(2-ethylhexyl) sulphosuccinate (AOT). Under the conditions we employ, the microemulsion consists of nanometre diameter droplets of water surrounded by a monolayer of AOT molecules, floating in a sea of oil. The average droplet diameter is proportional to the [water]/[AOT] ratio, while the distance between droplets increases with the [oil]/[water] ratio. Thus, by varying the composition of the microemulsion, one can tune its physical structure. Similarly, by modifying the concentrations of added BZ reactants, one can control the chemical properties of the system.

A key feature of the BZ–AOT system is that the BZ reactants are polar and thus tend to reside in the water droplets. The reaction does, however, produce non-polar intermediates, particularly Br_2 and BrO_2, which have a preference for the oil phase. This partitioning generates two different modes of diffusion in the system. Since the droplet diameter, 5–10 nm, is less than a diffusion length ($\cong (D\tau)^{1/2} \cong 0.1$ mm), diffusion within a droplet plays no role. Polar molecules diffuse via the random motion, collision, merging and redispersion of droplets, a process slower by an order of magnitude or so than the diffusion of non-polar species, which diffuse through the oil as single molecules with typical diffusion coefficients of 2×10^{-5} cm^2 s^{-1}. Another interesting aspect of this system is that, while a mature microemulsion with BZ reactants shows a single, relatively narrow peak in the distribution of droplet radii, the initial droplet distribution for the first few hours after mixing is bimodal, with peaks at about 5 and 20 nm, which eventually coalesce into a single peak just above the smaller maximum in the bimodal distribution. This behaviour is illustrated in figure 7. One may view the behaviour of the initial system at one level as that of a very large number of coupled droplets or, at a much coarser level, as arising from the interaction between populations of large and small droplets.

As one varies the physical and chemical properties of the BZ–AOT system, one observes a rich variety of patterns, many of which have not previously been seen in simpler reaction–diffusion systems. An overview of the spatio-

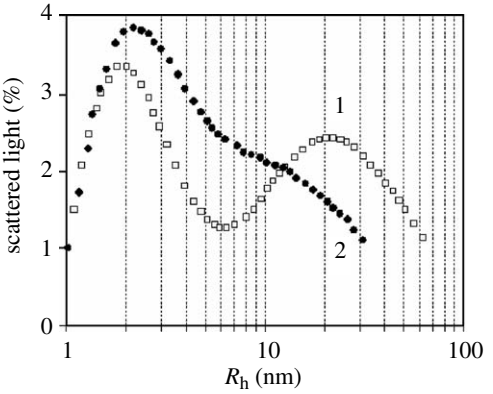

Figure 7. Distribution of droplet radii in a BZ–AOT microemulsion as measured by dynamic light scattering. Curve 1 shows a freshly prepared microemulsion. Curve 2 shows the same microemulsion after 24 h. Adapted from Vanag & Epstein (2003*a*).

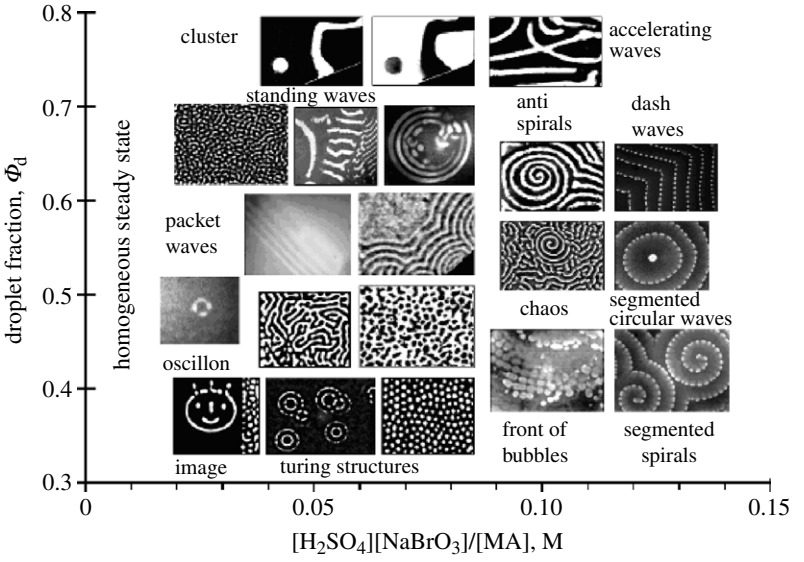

Figure 8. Overview of pattern formation in the BZ–AOT system as the compositions of the microemulsion and the BZ reactants are varied. Φ_d is the fraction of the total microemulsion volume occupied by the droplets.

temporal behaviour is shown in figure 8 where the horizontal axis represents the varying chemical composition of the BZ system and the vertical axis characterizes the physical state of the microemulsion. Among the patterns that differ from those seen in the aqueous BZ reaction are: the antispirals (Vanag & Epstein 2001*a*), in which the waves move towards rather than away from the centre of each spiral; the accelerating waves (Vanag & Epstein 2001*b*), which speed up just before collision and then move off perpendicular to the initial direction of approach, instead of maintaining a constant velocity and then annihilating on collision; and the Turing patterns (Vanag & Epstein 2001*b*), which arise owing to the existence of the two very different diffusion rates.

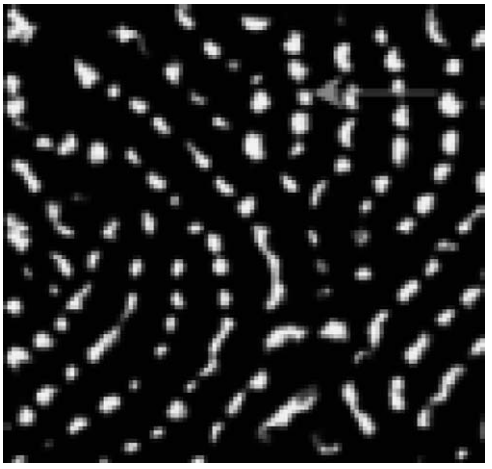

Figure 9. Dash waves in the ferroin-catalysed BZ–AOT system. Arrows show direction of motion of lines of waves. Frame size, 2.00×1.88 mm; velocity, 1.5–2 μm s^{-1}. Adapted from Vanag & Epstein (2003*a*).

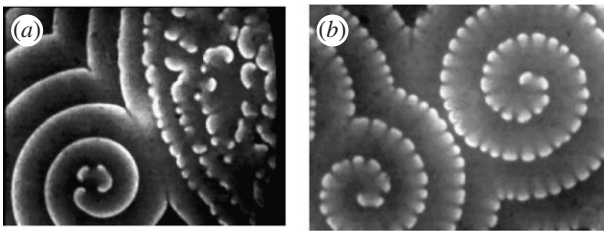

Figure 10. Segmented spirals in the BZ–AOT system. (*a*) Approach of dash waves (right) to a regular spiral (left), which is just beginning to segment into dashes near its centre. (*b*) Fully developed pair of segmented spirals. Adapted from Vanag & Epstein (2003*b*).

The dash waves, shown in more detail in figure 9, occur only in freshly prepared systems, i.e. they require two populations of droplet sizes. A related phenomenon, illustrated in figure 10, is the emergence of segmented spirals (Vanag & Epstein 2003*b*), which sometimes arise when dash waves approach an ordinary spiral.

(*c*) *Other BZ-based systems*

By a clever choice of the medium, one can produce coupling between patterns in other configurations involving the BZ reaction. Zhabotinsky *et al.* (1990) demonstrated that a BZ system in a layer of silica gel generates separate waves at the upper and lower surfaces, which then interact through the bulk of the gel.

Winston *et al.* (1991) impregnated a Nafion membrane with the BZ catalyst and then placed the membrane in a solution of the remaining BZ reactants. Patterns developed on both faces of the membrane. The patterns were initially independent of one another, but began to interact as the coupling between faces via passage of molecules through the membrane came into play. The strength of the coupling could be varied by changing the loading of the ferroin catalyst. With higher concentrations of ferroin, the coupling becomes weaker, as the $HBrO_2$ molecules

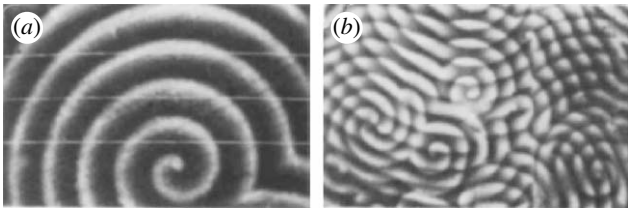

Figure 11. Spiral patterns observed on a Nafion membrane containing ferroin catalyst and immersed in a solution of BZ reactants. Image captures both front and back faces of the membrane. (*a*) Strong coupling, ferroin loading to 16.7% capacity and (*b*) weak coupling, loading to 38.7% capacity. Membrane thickness, 0.18 mm. Area shown is 6.2×4.7 mm. Adapted from Winston *et al.* (1991).

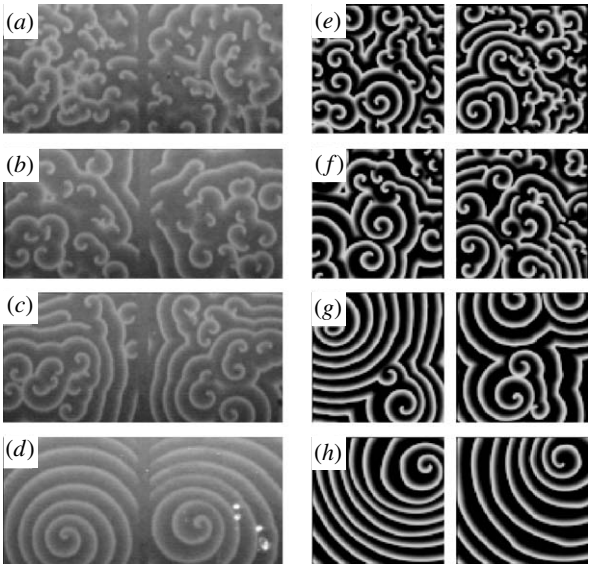

Figure 12. Synchronization of two photochemically coupled BZ patterns. (*a–d*) Experimental, time=(*a*) 2.30 min, (*b*) 12.25 min, (*c*) 30.00 min and (*d*) 76.52 min. Field of illumination, 7.13×3.51 cm, was divided into 362×167 square cells whose illumination level was updated every 2.0 s. (*e–h*) Computer simulation using two coupled Oregonator models (Tyson & Fife 1980). Adapted from Hildebrand *et al.* (2003).

responsible for the coupling have more difficulty travelling across the membrane. Figure 11 shows examples of both strong and weak coupling. With strong coupling, the two patterns are in almost perfect register, while with weaker coupling, the spiral patterns on the two faces behave nearly independently.

Using a somewhat more artificial, but much more controllable, technique, Hildebrand *et al.* (2003) coupled two photosensitive aqueous BZ systems in a pixel-by-pixel fashion. The two cells were illuminated and monitored using a video camera–projector scheme that made it possible to modify the level of illumination in each cell according to the difference in concentration of oxidized catalyst (a ruthenium bipyridyl complex) at corresponding locations in the two cells. In most cases, this symmetric coupling resulted in nearly but not quite perfect synchronization between the two initially independent patterns. Experimental results and a computer simulation are shown in figure 12.

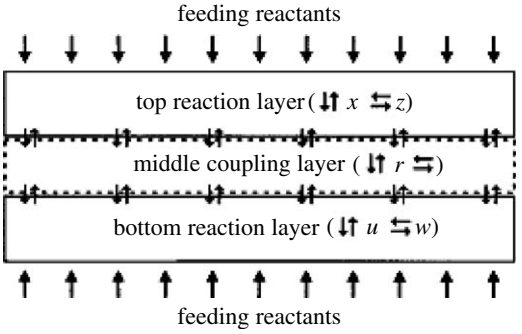

Figure 13. Schematic of a system consisting of two coupled layers with feeding, described by equations (3.1)–(3.5). Adapted from Yang & Epstein (2003).

3. Coupled patterns: simulations

One might imagine any number of ways of attempting to model the behaviour of coupled patterns, depending on the geometry of the system and the nature of the coupling. In many cases, however, the problem is relatively straightforward if one has at hand a reasonable model for each of the uncoupled subsystems and some understanding of how they are coupled. If each subsystem is described by a set of partial differential equations, one simply combines the equations for each of the subsystems and then augments the equations for any variable affected by the coupling with the appropriate coupling terms. A slightly more elaborate model (Yang & Epstein 2003) is shown in figure 13, where we imagine two layers, each containing two reactants x and z, coupled through a middle layer permeable only to x. The coupling is assumed to be diffusive in that it is proportional to the difference in concentration between two adjacent layers. The system is described by equations (3.1)–(3.5) as follows:

$$\frac{\partial x}{\partial t} = D_x \nabla^2 x + F(x,z) - \frac{1}{\delta}(x-r), \tag{3.1}$$

$$\frac{\partial z}{\partial t} = D_z \nabla^2 z + G(x,z), \tag{3.2}$$

$$\frac{\partial r}{\partial t} = D_r \nabla^2 r + \frac{1}{\delta}(x-r) + \frac{1}{\delta}(u-r), \tag{3.3}$$

$$\frac{\partial u}{\partial t} = D_u \nabla^2 u + F(u,w) - \frac{1}{\delta}(u-r) \tag{3.4}$$

and

$$\frac{\partial w}{\partial t} = D_w \nabla^2 w + G(u,w), \tag{3.5}$$

where the functions F and G characterize the kinetics in each uncoupled system, including the input from and output to any reservoir; the coupling strength $1/\delta$ is inversely proportional to the thickness of the middle layer; the D values are

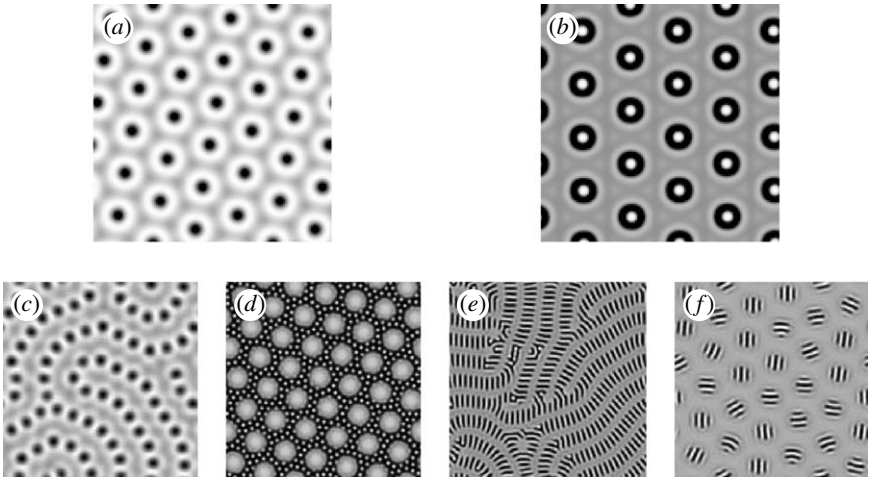

Figure 14. Simulations of coupled patterns using a Brusselator model for the functions F and G in equations (3.1) and (3.2). (a,b) Superlattice patterns. (c–f) Superposition patterns. Adapted from Yang *et al.* (2002).

diffusion coefficients; and u and w correspond to x and z, respectively, in the bottom layer, while r represents x in the middle layer.

Simulations of coupled layers can give rise to intricate and beautiful patterns, as illustrated in figure 14, where we show superlattice patterns obtained when the wavelengths of the subsystem patterns are in an appropriate ratio, and superposition patterns which appear when the two wavelengths are not related.

4. Forced systems: an example

Although there is a significant literature on forced patterns in both the BZ (e.g. Mikhailov & Showalter 2006) and the CDIMA (Dolnik *et al.* 2001; Berenstein *et al.* 2003) systems, we focus here on a single application of forcing in a photosensitive BZ–AOT system (Kaminaga *et al.* 2006). The unforced system shows bistability between stationary Turing patterns and a homogeneous steady state. The Turing patterns form spontaneously in the dark. At sufficiently high levels of illumination, I, the patterns disappear and only the homogeneous state is stable. In an intermediate range of I both states are stable, and which one appears depends upon the past history of the system. If we first illuminate the system at a high intensity through a mask to obliterate all patterns in the illuminated area and allow patterns to emerge or survive in the shadow regions and then illuminate the entire system at a lower intensity within the bistable range, we can produce an image of the mask in the reaction medium, as seen in figure 15*a*. Remarkably, because both the Turing pattern and the patternless homogeneous state are stable at this level of I, the pattern persists as seen in figure 15*b*, for an hour or more, close to the lifetime of the microemulsion. If we briefly raise I above the bistable range, the pattern disappears but reappears if we lower I back into that range. Longer exposures to high-intensity illumination permanently erase the pattern. Thus, we have a readable, writeable, erasable chemical memory!

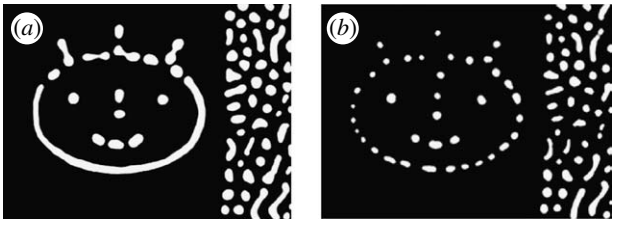

Figure 15. Images of a mask imprinted in the BZ–AOT reaction medium. Size of frames: 7.7× 5.8 mm. (*a*) Taken shortly after imprinting and (*b*) taken 1 hour later. Area at the right of each frame remains in the dark throughout the experiment. Adapted from Kaminaga *et al.* (2006).

5. Conclusion: future directions

We have seen that chemical systems provide convenient models for the study of coupled patterns and that qualitatively new kinds of patterns can emerge when spatio-temporal systems are coupled. Numerical simulation of coupled patterns is relatively straightforward, *if* one understands the uncoupled subsystems and the nature of the coupling between them. It would, however, be useful to have more powerful analytical techniques available to identify and analyse qualitatively different types of patterns and the bifurcation scenarios that lead from one to another.

We conclude with some brief speculations about promising directions for research in this field. First, it would be useful to have a complete catalogue of possible patterns, much as one can categorize the allowed types of temporal behaviour. As suggested above, it might then be worth seeking a theory, perhaps using the coupling strength as the key parameter, to understand the bifurcations between patterns. The notion of 'intelligent coupling' or 'feedback coupling', where the strength or even the form of the coupling evolves in response to the patterns formed, may be worth exploring. The example presented in §4 suggests that forced systems may have applicability towards building a 'chemical computer'. The BZ–AOT system in effect implements an earlier suggestion (Coullet *et al.* 2004) based on theoretical considerations that media of this type might provide a useful means of data storage. Other investigators (e.g. Gorecki *et al.* 2003) have used the BZ reaction to construct logic gates and other information processing elements. It is quite doubtful whether a computer of this type could compete with silicon-based devices, but it might provide a useful analogue for attempting to understand computation in living systems.

This work was supported by the National Science Foundation and the donors of the Petroleum Research Fund of the American Chemical Society.

References

Berenstein, I., Dolnik, M., Zhabotinsky, A. M. & Epstein, I. R. 2003 Spatial periodic perturbation of Turing pattern development using a striped mask. *J. Phys. Chem. A* **107**, 4428–4435. (doi:10.1021/jp026546k)

Berenstein, I., Dolnik, M., Yang, L. F., Zhabotinsky, A. M. & Epstein, I. R. 2004 Turing pattern formation in a two-layer system: superposition and superlattice patterns. *Phys. Rev. E* **70**, 046219, 1–5. (doi:10.1103/PhysRevE.70.046219)

Castets, V., Dulos, E., Boissonade, J. & De Kepper, P. 1990 Experimental evidence of a sustained standing Turing-type nonequilibrium chemical pattern. *Phys. Rev. Lett.* **64**, 2953–2956. (doi:10.1103/PhysRevLett.64.2953)

Coullet, P., Riera, C. & Tresser, C. 2004 A new approach to data storage using localized structures. *Chaos* **14**, 193–198. (doi:10.1063/1.1642311)

De Kepper, P., Epstein, I. R., Kustin, K. & Orbán, M. 1982 Batch oscillations and spatial wave patterns in chlorite oscillating systems. *J. Phys. Chem.* **86**, 170–171. (doi:10.1021/j100391a007)

Dolnik, M., Berenstein, I., Zhabotinsky, A. M. & Epstein, I. R. 2001 Spatial periodic forcing of Turing structures. *Phys. Rev. Lett.* **87**, 238301. (doi:10.1103/PhysRevLett.87.238301)

Gorecki, J., Yoshikawa, K. & Igarashi, Y. 2003 On chemical reactors that can count. *J. Phys. Chem. A* **107**, 1664–1669. (doi:10.1021/jp021041f)

Hildebrand, M., Cui, J. X., Mihaliuk, E., Wang, J. C. & Showalter, K. 2003 Synchronization of spatiotemporal patterns in locally coupled excitable media. *Phys. Rev. E* **68**, 026205. (doi:10.1103/PhysRevE.68.026205)

Kaminaga, A., Vanag, V. K. & Epstein, I. R. 2006 A reaction–diffusion memory device. *Angew. Chem. Int. Ed.* **45**, 3087–3089. (doi:10.1002/anie.200600400)

Lengyel, I. & Epstein, I. R. 1991 Modeling of Turing structures in the chlorite–iodide–malonic acid–starch reaction system. *Science* **251**, 650–652. (doi:10.1126/science.251.4994.650)

Lengyel, I., Rábai, G. & Epstein, I. R. 1990*a* Batch oscillation in the reaction of chlorine dioxide with iodine and malonic acid. *J. Am. Chem. Soc.* **112**, 4606–4607. (doi:10.1021/ja00167a103)

Lengyel, I., Rábai, G. & Epstein, I. R. 1990*b* Experimental and modeling study of oscillations in the chlorine dioxide–iodine–malonic acid reaction. *J. Am. Chem. Soc.* **112**, 9104–9110. (doi:10.1021/ja00181a011)

Mikhailov, A. S. & Showalter, K. 2006 Control of waves, patterns and turbulence in chemical systems. *Phys. Rep.* **425**, 79–194. (doi:10.1016/j.physrep.2005.11.003)

Turing, A. M. 1952 The chemical basis of morphogenesis. *Phil. Trans. R. Soc. B* **237**, 37–72. (doi:10.1098/rstb.1952.0012)

Tyson, J. J. & Fife, P. C. 1980 Target patterns in a realistic model of the Belousov–Zhabotinskii reaction. *J. Chem. Phys.* **73**, 2224–2237. (doi:10.1063/1.440418)

Vanag, V. K. & Epstein, I. R. 2001*a* Inwardly rotating spiral waves in a reaction–diffusion system. *Science* **294**, 835–837. (doi:10.1126/science.1064167)

Vanag, V. K. & Epstein, I. R. 2001*b* Pattern formation in a tunable reaction–diffusion medium: the BZ reaction in an aerosol OT microemulsion. *Phys. Rev. Lett.* **87**, 228301, 1–4. (doi:10.1103/PhysRevLett.87.228301)

Vanag, V. K. & Epstein, I. R. 2003*a* Dash-waves in a reaction–diffusion system. *Phys. Rev. Lett.* **90**, 098301, 1–4. (doi:10.1103/PhysRevLett.90.098301)

Vanag, V. K. & Epstein, I. R. 2003*b* Segmented spiral waves in a reaction–diffusion system. *Proc. Natl Acad. Sci. USA* **100**, 14 635–14 638. (doi:10.1073/pnas.2534816100)

Winston, D., Arora, M., Maselko, J., Gáspár, V. & Showalter, K. 1991 Cross membrane coupling of spatiotemporal patterns. *Nature* **351**, 132–135. (doi:10.1038/351132a0)

Yang, L. F. & Epstein, I. R. 2003 Oscillatory Turing patterns in reaction–diffusion systems with two coupled layers. *Phys. Rev. Lett.* **90**, 178303. (doi:10.1103/PhysRevLett.90.178303)

Yang, L., Dolnik, M., Zhabotinsky, A. M. & Epstein, I. R. 2002 Spatial resonances and superposition patterns in a reaction–diffusion model with interacting Turing modes. *Phys. Rev. Lett.* **88**, 208303. (doi:10.1103/PhysRevLett.88.208303)

Zhabotinsky, A. M., Müller, S. C. & Hess, B. 1990 Interaction of chemical waves in a thin layer of microheterogeneous gel with a transversal chemical gradient. *Chem. Phys. Lett.* **172**, 445–448. (doi:10.1016/0009-2614(90)80136-2)